

part, by acquiring several two-dimensional views. The plots in Fig. 2c, f and k indicate that ants may have adopted a strategy of sampling more often close to the cone, where image size changes rapidly, and less frequently further away, where image size is less dependent on range. Sampling the cone at equi-angular separations gives the ant a series of views that evenly covers the transformation of the shape from its first sighting to the ant's arrival at its base (Fig. 1e, f, g). □

Methods

Housing, training and testing ants. Ant nests were kept in large plastic tanks. Individually marked foragers collected sucrose on a flat shelf (120 cm by 80 cm) above the nest which they reached by means of a paper 'drawbridge' (Fig. 1a). Ants from one colony foraged for sucrose at the base of a black upright cone (7-cm base, 12-cm height). The cone was inverted for ants from another colony. Both cone types were present during the training for the choice experiment (Fig. 1) and the positions of the cones were swapped frequently. One cone was associated with the sucrose and the other was an unrewarded distractor. The shelf was wiped with alcohol after each foraging trip to remove possible trail pheromones.

Videorecording and analysis. The ~30-cm trips to and from the feeder were videorecorded from above and analysed automatically to obtain the ant's position and the orientation of its body axis. The retinal position of the edge of the cone was calculated on the assumption that the head is aligned with the body. High-magnification videorecordings of ants as they walked straight and turned corners showed that the head is kept mostly aligned with the body. On straight paths, the mean angle between head and body was 0.013° (s.d. = $\pm 1.99^\circ$, $n = 90$ frames), and while the ant was performing a 83° turn the mean angle between head and body was 2.57° (s.d. = $\pm 3.78^\circ$, $n = 23$ frames).

Plateaux were selected using a computer algorithm that fitted straight-line segments to the plots of the retinal position of edges. The plateaux collected from all the approaches made by one ant to the same stimulus were sorted into a histogram, which displays how long the edge was held in different retinal positions. Peaks in the histogram were then found using another computer algorithm. The data were first smoothed with a binomial filter of width 1, and the peak positions were given by the positions of the remaining local maxima.

Assessing the similarity of multimodal distributions. Statistical tests were performed on the data from each ant using the positions of the peaks. We compared the similarity of peak positions from approaches to cones and approaches to extended edges, or from departures from cones and approaches to extended edges. The computer picked out the closest matching pairs of peaks in the two distributions as follows: for any given peak in the edge-derived data, the closest peak in the cone-derived data was found. Provided that the reverse also held, that is, that the original peak in the edge-derived data was the closest peak to the matched peak in the cone-derived data, the interpeak difference was recorded and the pair was removed from the data set. This was continued until there were no further matches. The process was repeated with data from the other ants, and the standard deviation of all of the peak differences, assuming a mean difference of zero, was taken as a measure of the similarity of the distributions. The better the match between the peak distributions, the smaller this similarity score was.

5,000 sets of artificially generated cone-derived data were then matched to the real edge-derived data using the same procedure. For each ant, the artificial data sets each had the same number of peaks as the real data, but the peaks were distributed randomly between 0° and 80° from the midline, with the constraint of a minimum separation of 6° and a maximum separation of 24° between peaks. We computed a similarity score across all ants for each data set. The number of sets out of the 5,000 that scored less than the real data was taken as the probability of getting the real match by chance¹⁶.

Received 3 December 1997; accepted 19 February 1998.

- Dill, M., Wolf, R. & Heisenberg, M. Visual pattern recognition in *Drosophila* involves retinotopic matching. *Nature* **365**, 751–753 (1993).
- Wehner, R. in *Handbook of Sensory Physiology* Vol. VII/6C (ed. Autrum, H.) 287–616 (Springer, Berlin, Heidelberg, New York, 1981).
- Collett, T. S. & Land, M. F. Visual spatial memory in a hoverfly. *J. Comp. Physiol.* **100**, 59–84 (1975).
- Wehner, R. & Rüber, F. Visual spatial memory in desert ants, *Cataglyphis fortis* (Hymenoptera, Formicidae). *Experientia* **35**, 1569–1571 (1979).

- Cartwright, B. A. & Collett, T. S. Landmark learning in bees: experiments and models. *J. Comp. Physiol.* **151**, 521–543 (1983).
- Zollikofer, C. P. E., Wehner, R. & Fukushima, T. Optical scaling in conspecific *Cataglyphis* ants. *J. Exp. Biol.* **198**, 1637–1646 (1995).
- Vollbehre, J. Zur Orientierung junger Honigbienen bei ihrem ersten Orientierungsflug. *Zool. Jb.* **79**, 33–69 (1975).
- Zeil, J. Orientation flights of solitary wasps (*Cerceris*; Sphecidae; Hymenoptera): I. Description of flight. *J. Comp. Physiol.* **A172**, 189–205 (1993).
- Lehrer, M. Why do bees turn back and look? *J. Comp. Physiol.* **A172**, 549–563 (1993).
- Collett, T. S. & Lehrer, M. Looking and learning: a spatial pattern in the orientation flight of the wasp *Vespa vulgaris*. *Proc. R. Soc. Lond. B* **252**, 129–134 (1993).
- Rock, I., DiVita, J. & Barbeito, R. The effect on form perception of change of orientation in the third dimension. *J. Exp. Psychol. Hum. Percept. Perform.* **7**, 719–732 (1981).
- Rock, I. & DiVita, J. A case of viewer centred object perception. *Cogn. Psychol.* **19**, 280–293 (1987).
- Tarr, M. J. & Pinker, S. Mental rotation and orientation-dependence in shape recognition. *Cogn. Psychol.* **21**, 233–282 (1989).
- Bülthoff, H. H. & Edelman, S. Psychophysical support for a two-dimensional view interpolation theory of object recognition. *Proc. Natl Acad. Sci. USA* **89**, 60–64 (1992).
- Ullman, S. *High Level Vision: Object Recognition and Visual Cognition* (MIT Press, Cambridge, MA, 1996).
- Manly, B. F. J. *Randomization and Monte Carlo Methods in Biology* (Chapman and Hall, London, 1991).

Acknowledgements. We thank M. F. Land and D. Osorio for valuable comments. Financial support came from the BBSRC and Human Frontier Science Program. S.P.D.J. received a BBSRC research studentship.

Correspondence and requests for materials should be addressed to S.P.D.J. or T.S.C.

Encoding of three-dimensional structure-from-motion by primate area MT neurons

David C. Bradley, Grace C. Chang & Richard A. Andersen

Division of Biology, California Institute of Technology,
391 South Holliston Avenue, Pasadena, California 91125, USA

We see the world as three-dimensional, but because the retinal image is flat, we must derive the third dimension, depth, from two-dimensional cues. Image movement provides one of the most potent cues for depth^{1–6}. For example, the shadow of a contorted wire appears flat when the wire is stationary, but rotating the wire causes motion in the shadow, which suddenly appears three-dimensional. The neural mechanism of this effect, known as 'structure-from-motion', has not been discovered. Here we study cortical area MT, a primate region that is involved in visual motion perception. Two rhesus monkeys were trained to fixate their gaze while viewing two-dimensional projections of transparent, revolving cylinders. These stimuli appear to be three-dimensional, but the surface order perceived (front as opposed to back) tends to reverse spontaneously. These reversals occur because the stimulus does not specify which surface is in front or at the back. Monkeys reported which surface order they perceived after viewing the stimulus. In many of the neurons tested, there was a reproducible change in activity that coincided with reversals of the perceived surface order, even though the stimulus remained identical. This suggests that area MT has a basic role in structure-from-motion perception.

We trained two rhesus monkeys to fixate on a stationary target while we showed the two-dimensional projection of a revolving, random-dot cylinder (Fig. 1a). This projection contains opposite-going motions which convey a sense of front and back, or surface order. Monkeys then reported the direction of the front surface by glancing at one of two targets that appeared on either side of the cylinder's former position. As two-dimensional projections are flat, they do not specify the surface order, so the monkeys' answers reflect their three-dimensional perception of the stimulus.

We also showed rotating cylinders whose structure (and thus surface order) was specified with disparity (depth). Some of these were flattened by multiplying the depth of each dot by a fraction (0, 12.5, 25, 50 or 100%). All cylinders had their centre at zero disparity, so one surface appeared to be near, the other far, relative to the

fixation depth. Figure 1b shows that performance—the ability to judge surface order—decreased predictably as the disparity decreased, suggesting that monkeys were doing the task as required.

In simultaneous, single-neuron recordings of MT activity, we oriented cylinders so that one surface moved in the neuron's preferred direction (determined in preliminary tests), the other in the opposite direction. We expected responses to depend on surface order because MT cells tend to prefer motion either behind or in front of the fixation point (far or near)⁷. Preferred-direction motion on the 'active' side tends to excite, whereas antipreferred motion on the active side tends to suppress⁸. Therefore, one of the two surface orders should be optimal because it places preferred motion on the active side while placing antipreferred motion on the other side. Indeed, when the highest-disparity cylinders were shown, 68/109 MT cells responded significantly better to one of the two surface orders ($P < 0.05$, t -test).

Responses were linked to the perception of surface order. The cell in Fig. 2, for example, preferred the front going down, the back up, and this was true whether that surface order was specified with disparity (top) or simply perceived as such in a zero-disparity stimulus (bottom). Of the 68 cells with a preferred surface order (see above), 34 responded differently when the stimulus was perceived with different surface orders ($P < 0.05$, t -test; see Methods). Most cells (27/34) showed 'correlated' behaviour, meaning that responses were higher when the neuron's preferred order (defined at the highest disparity) was perceived. This was true for both types of cells irrespective of whether they had a preferred direction in front (17/20) or in the back (7/9; 5 cells not classifiable

as near or far). Given the low frequency of cells with the opposite behaviour (7 of 68 possible), it is not clear whether a distinct cell class of this type really exists.

Although disparity cues bias perception in favour of a particular surface order, all stimuli were potentially bistable (could be perceived either way) (Fig. 1b). Figure 3a shows that whatever the disparity, and whatever the specified surface order, responses were higher when the neuron's preferred surface order was perceived (compared with the non-preferred order). Moreover, whether the variable was the specified surface order (100% disparity) or the perceived surface order (zero disparity), the time course over which activity diverged was similar (Fig. 3b). Thus, to the extent that the perceived surface order of a given stimulus differed, MT activities tended to reflect that difference.

Previous experiments with flat patterns showed that opposite motion directions suppress MT responses, but that this suppression decreases, and in some cases changes to facilitation, when opposite directions are shown at different disparities^{8,9}. This suggests that there are inhibitory connections between MT cells tuned for opposite directions and similar depths (Fig. 4a), and excitatory connections between cells tuned for opposite directions and different depths (that is, near rather than far). Such depth-dependent interactions may be important for computing surface movement because they emphasize coherent (same direction) motion signals while suppressing random signals (motion noise) from a given surface^{8,10}.

Structure-from-motion perception may begin with the bistable nature of this circuitry. MT cells typically prefer either near or far

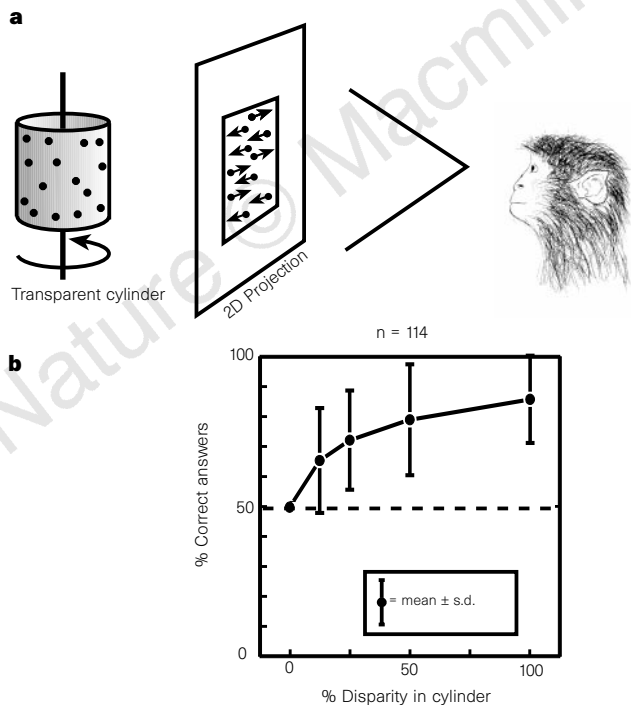


Figure 1 The monkeys' task and average performance. **a**, Monkeys viewed two-dimensional projections of three-dimensional, revolving cylinders, then reported the direction of rotation they perceived. **b**, Psychometric function (all data pooled and averaged) relating performance to the amount of disparity in the cylinders. The abscissa shows disparity as a percentage of the disparity that would be seen looking at a real (3D) cylinder. The ordinate shows the percentage of correct answers regarding the surface order. Error bars show standard deviation.

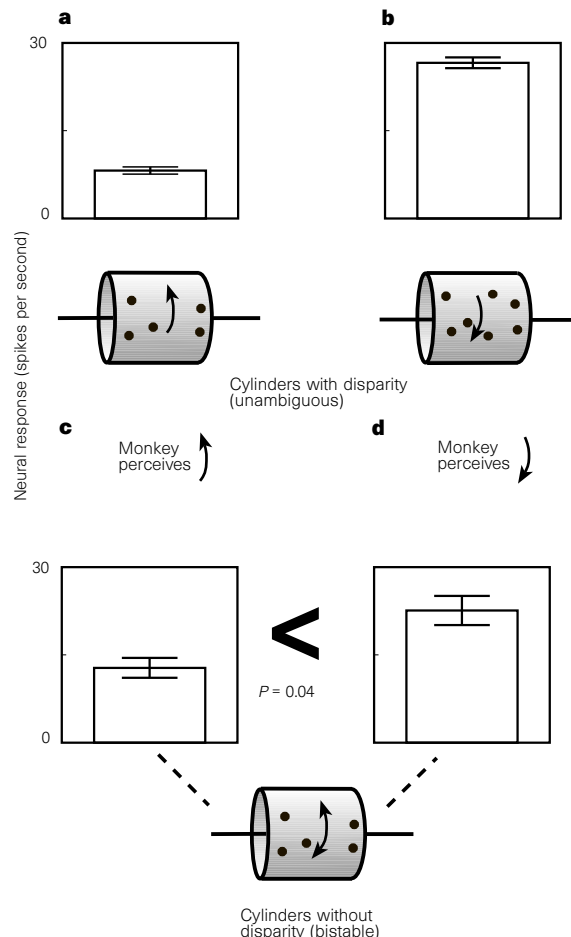


Figure 2 Data from an MT neuron. **a, b**, Responses to 100%-disparity cylinders (using only trials with correct responses). **c, d**, Responses of the same cell to zero-disparity cylinders, perceived as going front-up (**c**) or front-down (**d**).

stimuli, but their tuning is broad enough that they also respond to zero-disparity stimuli⁷. Therefore, a zero-disparity cylinder projection could potentially activate four neuronal pools, tuned (assuming a vertical cylinder) for near-right, near-left, far-right and far-left (Fig. 4a). But because of the inhibition and excitation discussed above, an even distribution of activity would be unstable, tending to 'fall' into a distribution that places opposite directions in different depth channels. For example, an increase in the activity of near-right cells could lead to a suppression of near-left cells and an activation of far-left cells; the far-left cells, in turn, would suppress the far-right cells, and so on. The resulting activity distribution would be concentrated in the near-right and far-left channels, presumably resulting in the perception of the front surface moving right, the back moving left (Fig. 4b). On different trials, activity might instead end up in the near-left and far-right channels, depending on the adaptation, or fatigue, of the different channels at the outset of each trial¹¹.

In some MT neurons, activity increases when the monkey pays attention to that neuron's preferred direction¹². Assuming our monkeys always attended the cylinder's front surface, this could produce an artefact by increasing activity when the neuron's preferred direction appears in front. However, many neurons responded best when their preferred direction was in the back. Moreover, when a neuron preferred a given surface order (based on

disparity), it typically responded best when that order was perceived. This cannot be explained by an attention effect, unless the monkeys learned selectively to attend to one of the two surfaces, depending on the response properties of the neuron currently being tested. This is extremely unlikely.

Area MT is no doubt specialized for motion computation^{13,14}, but there is accumulating evidence that it also has a role in three-dimensional surface representation. MT neurons have large receptive fields, capable of spatially integrating motion cues; they are direction- and depth-selective, consistent with surface-oriented motion computation; and they exhibit direction opponency, which may be used for surface-specific noise reduction^{7-10,15}. MT neurons are thus well suited to the task of transforming motion cues into information about surfaces and depth. In fact, MT lesions impair monkeys in tasks where three-dimensional structure is judged from motion cues^{5,6}. Up to now, however, there has been no direct evidence that the perception of structure is linked to activities in MT. Our findings provide this evidence, and as such they suggest that MT has a central role in structure-from-motion perception. Of course, perception may occur in a different area which receives input from MT. But wherever it occurs, our findings indicate that the perception of structure is ultimately influenced by the segregation of MT activity into separate depth channels. □

Methods

Stimuli. Visual stimuli were shown on a 21-inch CRT screen, 57 cm from the monkey's eyes. Isolated neurons were tested to find their approximate receptive field, and subsequent stimuli were centred within this field. Neurons were tested for single-pattern direction selectivity as described⁸.

Cylinder projections were 7° wide and 7° tall, contained 150 randomly placed dots⁸, and rotated at 100° per second. Cylinders were positioned with their centre 3.0–8.2° from the fixation point, and with 10/109 exceptions, no part of the cylinder overlapped the fixation point. All cylinders had their centre at zero disparity, so one surface appeared near, the other far, relative to the fixation depth. Dots were rendered in stereo with an anaglyph system⁸.

Most neurons were tested with cylinders containing 5 disparity levels (0, 12.5, 25, 50 and 100%) as explained in the text. However, in preliminary tests with 31 of the neurons, only two disparities were tested: one low (0 or 12.5%) and one high (25–100%). Results from these cells were similar to those overall, so they were combined with the remaining cells to form the present data set.

Task. Monkeys fixated for 0.5 s before, 1 s during, and 0.5 s after the 1-s cylinder presentation. Selection targets were 5.5° on either side of the cylinder's rotation axis, positioned on a line bisecting the cylinder's height. Monkeys were rewarded with a drop of juice for choosing the target corresponding to the direction of the front surface (for zero-disparity cylinders, rewards were given randomly at a frequency of 80%).

Eye position. Monkeys were required to fixate within a 3° square window while the cylinder appeared on the screen. Subsequent analysis showed that eye position remained inside a 1° window in 97% of the trials. The within-trial standard deviation of eye position, sampled at 100 Hz, was 0.05° horizontal, 0.12° vertical.

In one of the monkeys, both eye positions were measured simultaneously to calculate the depth of fixation (units of degrees angular disparity). Standard deviation was 0.05° within trials and 0.07° from trial-to-trial. Comparing trials in which opposite surface orders were perceived revealed no differences in fixation depth ($P \geq 0.05$ in 95% of the t -tests; $n = 53$).

Analysis. Our main analysis involved testing for a response difference ($P < 0.05$, t -test) associated with the perceived surface order of one or more of the stimuli (each stimulus defined by a given disparity and surface order). Multiple t -testing can in theory increase the false-positive rate, but it cannot account for the high percentage of 'correlated' cells (see text), because false positives have an even chance of being correlated.

Received 4 August 1997; accepted 20 January 1998.

1. Rogers, B. J. & Graham, M. E. Similarities between motion parallax and stereopsis in human depth perception. *Vision Res.* **22**, 261–270 (1982).
2. Miles, W. R. Movement interpretations of the silhouette of a revolving fan. *Am. J. Psychol.* **43**, 392–405 (1931).
3. Wallach, H. & O'Connell, D. N. The kinetic depth effect. *J. Exp. Psychol.* **45**, 205–217 (1953).

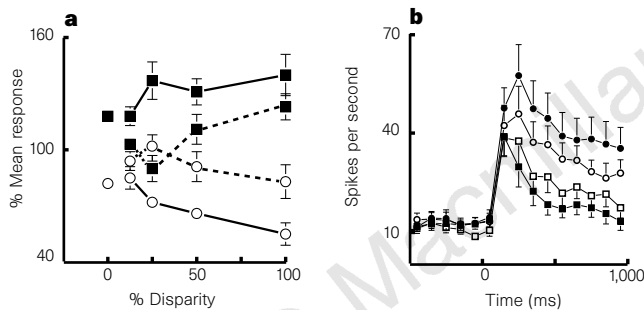


Figure 3 Averaged data from 'correlated' MT cells ($n = 27$). **a**, Perceptual effects at different disparities. Responses were normalized to the mean response for each disparity and plotted as a function of disparity. Data show mean responses \pm standard error. Top two curves (squares): actual surface order matches the neuron's preferred surface order. Lower two curves (circles): actual surface order is opposite to the neuron's preferred order. Solid lines, correct trials; broken lines, error trials. At zero disparity, as there is no actual surface order (the stimulus has zero disparity), the data points represent the two perceived surface orders. **b**, Time course of responses at zero disparity (inner traces) and 100% disparity (outer traces; correct trials only). Circles represent the neurons' preferred surface order (perceived or actual); squares represent the non-preferred order. The stimulus was visible from 0–1,000 ms. Data show mean response \pm standard error (in some cases error bars are smaller than the symbols).

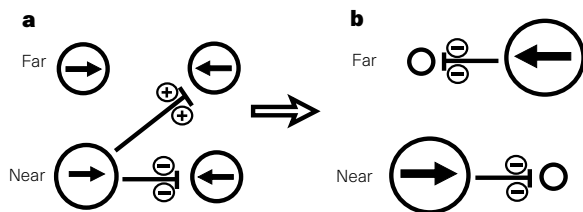


Figure 4 Proposed model to explain how suppression and facilitation in MT could give rise to the illusion of depth: **a**, a cylinder projection could activate four neuronal pools; **b**, because of excitatory and inhibitory interactions, activity migrates into opposite-direction, separate-depth channels. This presumably creates the perception of a cylinder rotating in a single direction. Circle diameter denotes magnitude of activity.

4. Ringach, D. L., Hawken, M. J. & Shapley, R. Binocular eye-movements caused by the perception of 3-dimensional structure-from-motion. *Vision Res.* **36**, 1479–1492 (1996).
5. Siegel, R. M. & Andersen, R. A. Perception of three-dimensional structure from motion in monkey and man. *Nature* **331**, 259–261 (1988).
6. Andersen, R. A. & Siegel, R. M. in *Signal and Sense: Local and Global Order in Perceptual Maps* (eds Edelman, G. M., Gall, W. E. & Cowan, W. M.) 163–184 (Wiley, New York, 1990).
7. Maunsell, J. H. & Van Essen, D. C. Functional properties of neurons in middle temporal visual area of the macaque monkey. II. Binocular interactions and sensitivity to binocular disparity. *J. Neurophysiol.* **49**, 1148–1167 (1983).
8. Bradley, D. C., Qian, N. & Andersen, R. A. Integration of motion and stereopsis in middle temporal cortical area of macaques. *Nature* **373**, 609–611 (1995).
9. Snowden, R. J., Treue, S., Erickson, R. G. & Andersen, R. A. The response of area MT and V1 neurons to transparent motion. *J. Neurosci.* **11**, 2768–2785 (1991).
10. Hildreth, E. C., Ando, H., Andersen, R. A. & Treue, S. Recovering three-dimensional structure from motion with surface reconstruction. *Vision Res.* **35**, 117–137 (1995).
11. Nawrot, M. & Blake, R. A neural network model of kinetic depth. *Visual Neurosci.* **6**, 219–227 (1991).
12. Treue, S. & Maunsell, J. H. R. Attentional modulation of visual-motion processing in cortical areas MT and MST. *Nature* **382**, 539–541 (1996).
13. Newsome, W. T., Britten, K. H. & Movshon, J. A. Neuronal correlates of a perceptual decision. *Nature* **341**, 52–54 (1989).
14. Logothetis, N. K. & Schall, J. D. Neuronal correlates of subjective visual perception. *Science* **245**, 761–763 (1989).
15. Braddick, O. Segmentation versus integration in visual-motion processing. *Trends Neurosci.* **16**, 263–268 (1993).

Acknowledgements. We thank B. Gillikin and S. Gertmenian for technical assistance and F. Crick and C. Koch for comments on the manuscript. Supported by grants from the National Eye Institute, the Human Frontier Science Program, and the Sloan Foundation for Theoretical Neurobiology.

Correspondence and requests for material should be addressed to R.A.A. (e-mail: andersen@vis.caltech.edu).

Glycine-receptor activation is required for receptor clustering in spinal neurons

J. Kirsch & H. Betz

Department of Neurochemistry, Max-Planck-Institute for Brain Research, Deutscherordenstrasse 46, 60528 Frankfurt/Main, Germany

The ability of nerve cells to receive up to several thousands of synaptic inputs from other neurons provides the anatomical basis for information processing in the vertebrate brain. The formation of functional synapses involves selective clustering of neurotransmitter receptors at presumptive postsynaptic regions of the neuronal plasma membrane^{1–4}. Receptor-associated proteins are believed to be crucial for this process. In spinal neurons, synaptic

targeting of the inhibitory glycine receptor (GlyR)^{5,6} depends on the expression of the anchoring protein gephyrin^{7–9}. Here we show that the competitive GlyR antagonist strychnine and L-type Ca²⁺-channel blockers inhibit the accumulation of GlyR and gephyrin at postsynaptic membrane areas in cultured rat spinal neurons. Our data are consistent with a model in which GlyR activation that results in Ca²⁺ influx is required for the clustering of gephyrin and GlyR at developing postsynaptic sites. Similar activity-driven mechanisms may be of general importance in synaptogenesis.

Inhibitory neurotransmission in adult spinal cord is largely mediated by the strychnine-sensitive glycine receptor GlyR¹⁰. The developmental sequence of GlyR expression is recapitulated in primary cultures prepared from rodent spinal cord at embryonic day 14 (refs 11, 12). After 6–10 days *in vitro*, more than 90% of the neurons in these cultures express functional glycine receptors^{9,13,14}. By using double labelling with the GlyR-specific monoclonal antibody 4a (ref. 15) and a polyclonal antibody raised against synaptic vesicle proteins (anti-SVP)¹⁶, it has been shown that synaptic contacts between neurons that are characterized by the close apposition of pre- and postsynaptic antigens are established after one week in culture^{9,14}. We find that early treatment (within 24 h of plating) of rat spinal cord cultures with 30 μM tetrodotoxin, which blocks neuronal activity by inhibiting voltage-dependent Na⁺ channels, prevents formation of postsynaptic GlyR clusters (data not shown). To determine whether activation of GlyR could be responsible for this activity dependence, we added the competitive antagonist strychnine to the culture medium: this did not affect the formation of neurites and nerve terminals enriched in synaptic vesicle antigens, but the number of GlyR clusters was markedly reduced and immunoreactivity of antibody 4a was evident in large intracellular structures that could be endosomes (Fig. 1a). Likewise, the GlyR-associated peripheral membrane protein gephyrin revealed by monoclonal antibody 7a (ref. 15) was no longer detected at postsynaptic sites after strychnine treatment but was seen instead at sites of focal cell attachment (Fig. 1b), as described for the early stages in development⁹. The overall content of GlyR and gephyrin was not reduced by addition of strychnine, as shown by dot immunoassay (Fig. 1c, d). Inhibition of GlyR clustering by strychnine was reversible after washout of strychnine at day 8 *in vitro*, and if strychnine was added after 8 days *in vitro*, when GlyR clusters had already formed, the postsynaptic localization of antigens detected

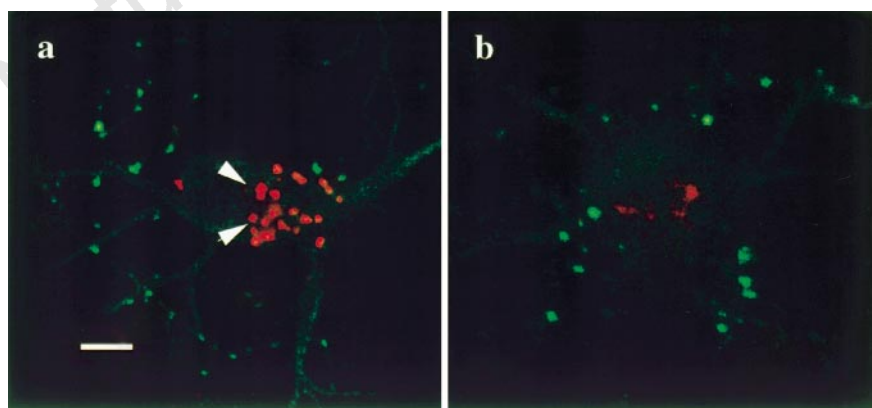


Figure 1 Effect of strychnine treatment on the distribution of GlyR and gephyrin in spinal cultures.

a, b, Confocal optical sections of embryonic spinal cord neurons cultured for 8 days in the presence of 0.5 μM strychnine. Cells were doubly immunolabelled with anti-SVP (green) and monoclonal antibodies (mAbs) 4a (red; **a**) or 7a (red; **b**). Upon strychnine treatment, mAb 4a immunoreactivity was confined to large intracellular structures (**a**, arrowheads), whereas mAb 7a immunoreactivity was concentrated at intracellular sites close to the substrate (**b**). For controls, see ref. 14. Scale bar: 5 μm. **c, d**, GlyR and gephyrin protein levels in strychnine-treated and control cultures. The amounts of GlyR (**c**) and gephyrin (**d**), determined by mAb 4a or 7a dot immunoassay, in cultures treated with 0.05 μM (light grey bars), 0.1 μM (white bars) or 0.5 μM (dark grey bars) strychnine were not significantly different from those in control cultures (black bars).

